First-principles materials design for semiconductor spintronics

Application of MACHIKANEYAMA
to materials design

K. Sato, Osaka Univ.
T. Fukushima, Univ. of Tokyo

CMD36 workshop
28, Feb. 2020. Osaka Univ. Toyonaka

OUTLINE

- **Introduction**
  - Spintronics, dilute magnetic semiconductors (DMS)
  - Why we need MACHIKANEYAMA ?
    - Disordered systems
    - Finite temperature magnetism
- **Dilute magnetic semiconductors**
  - Origin of the ferromagnetism in DMS
  - Magnetic interactions in DMS
  - Practical and accurate T_C calculation for DMS
  - **Why high-T_C is so difficult ?**
- **Inhomogeneity in DMS**

K. Sato et al.,
First-principles theory of dilute magnetic semiconductors, Rev. Mod. Phys., 82 (2010) 1633.
T. Dietl et al.,
Spinodal nanodecomposition in semiconductors doped with magnetic impurities, Rev. Mod. Phys. 87 (2015) 1311.

SPINTRONICS AND DILUTE MAGNETIC SEMICONDUCTORS

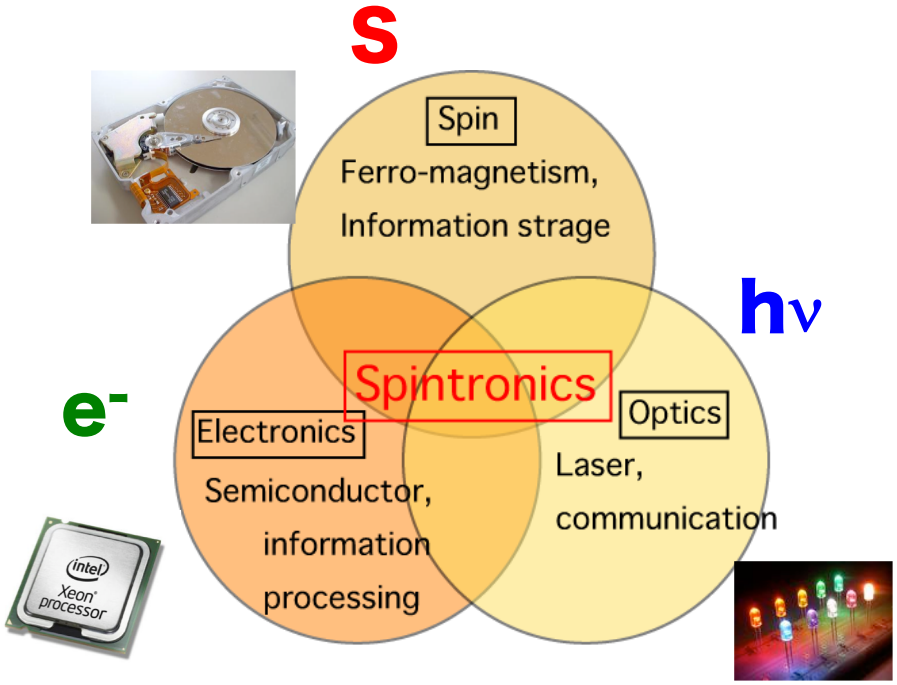

References:
G. A. Prinz, Science 282 (1998) 1660. H. Ohno, JMMM 200 (1999
S. A. Wolf, Science 294 (2001) 1488. T. Dietl, Semicond. Sci. Tec

(Ga, Mn)As

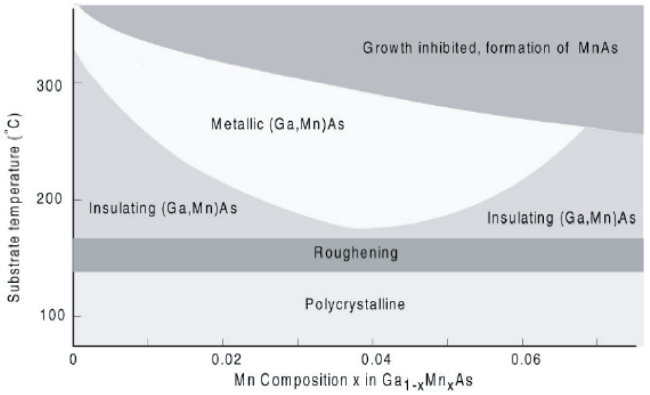

Fig. 1. Schematic phase diagram showing the relation between growth parameters (substrate temperature and Mn concentration) and the properties of (Ga,Mn)As grown by molecular beam epitaxy.

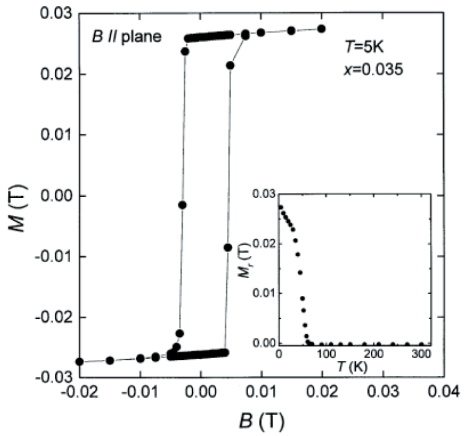

Fig. 3. Magnetic field dependence of magnetization M at 5 K for a (Ga,Mn)As film with Mn content $x = 0.035$. The field was applied parallel to the sample surface. Inset shows the temperature dependence of the remanent magnetization M_r of the same sample.

- Dilute magnetic semiconductor (DMS)
- Carrier induced ferromagnetism
  - (In, Mn)As; T_C = 60 (K)
  - (Ga, Mn)As; T_C = 190 (K)

'Properties of ferromagnetic III-V semiconductors'
H. Ohno, J. Magn. Magn. Matt. 200 (1999) 110.

ELECTRIC-FIELD CONTROL OF FERROMAGNETISM IN (In, Mn)As

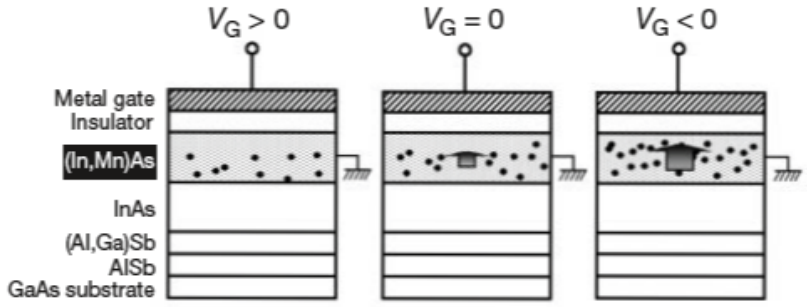

Figure 1 Field-effect control of the hole-induced ferromagnetism in magnetic semiconductor (In,Mn)As field-effect transistors. Shown are the cross-sections of a metal-insulator–semiconductor structure under gate biases V_G. This controls the hole concentration in the magnetic semiconductor channel (filled circles). Negative V_G increases hole concentration, resulting in enhancement of the ferromagnetic interaction among magnetic Mn ions, whereas positive V_G has an opposite effect. The arrow schematically shows the magnitude of the Mn magnetization. The InAs/(Al,Ga)Sb/AlSb structure under the (In,Mn)As layer serves as a buffer relaxing the lattice mismatch between the structure and the GaAs substrate to produce a smooth surface on which the magnetic layer is grown.

'Electric-field control of ferromagnetism'
H. Ohno et al. Nature 408 (2000) 944.

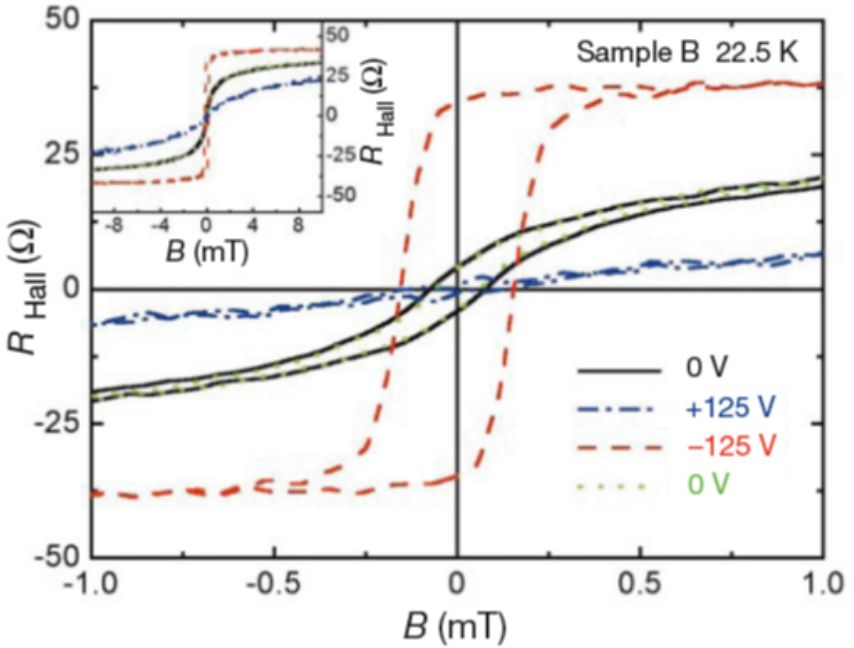

Figure 3 R_{Hall} versus field curves under three different gate biases. Application of $V_G = 0$, +125 and −125 V results in qualitatively different field dependence of R_{Hall} measured at 22.5 K (sample B). When holes are partially depleted from the channel ($V_G = +125$ V), a paramagnetic response is observed (blue dash-dotted line), whereas a clear hysteresis at low fields (<0.7 mT) appears as holes are accumulated in the channel ($V_G = -125$ V, red dashed line). Two R_{Hall} curves measured at $V_G = 0$ V before and after application of ±125 V (black solid line and green dotted line, respectively) are virtually identical. Inset, the same curves shown at higher magnetic fields.

ELECTRICAL SPIN INJECTION

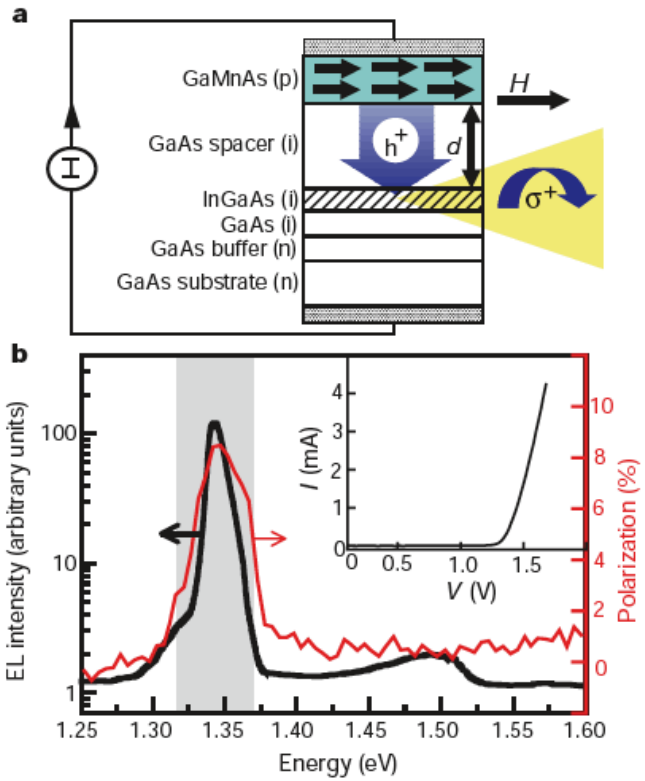

Figure 1 Electrical spin injection in an epitaxially grown ferromagnetic semiconductor heterostructure, based on GaAs. **a**, Spontaneous magnitization develops below the Curie temperature T_C in the ferromagnetic p-type semiconductor (Ga,Mn)As, depicted by the black arrows in the green layer. Under forward bias, spin-polarized holes from (Ga,Mn)As and unpolarized electrons from the n-type GaAs substrate are injected into the (In,Ga)As quantum well (QW, hatched region), through a spacer layer with thickness d, producing polarized EL. **b**, Total electroluminescence (EL) intensity of the device ($d = 20$ nm) under forward bias at temperature $T = 6$ K and magnetic field $H = 1{,}000$ Oe is shown (black curve) with its corresponding polarization (red curve). Current $I = 1.43$ mA. Note that the polarization is largest at the QW ground state ($E = 1.34$ eV). The EL and polarization are plotted on semi-log and linear scales, respectively. Inset, a current–voltage plot characteristic of a 20-nm spacer layer device. Shaded grey area, see Fig. 2.

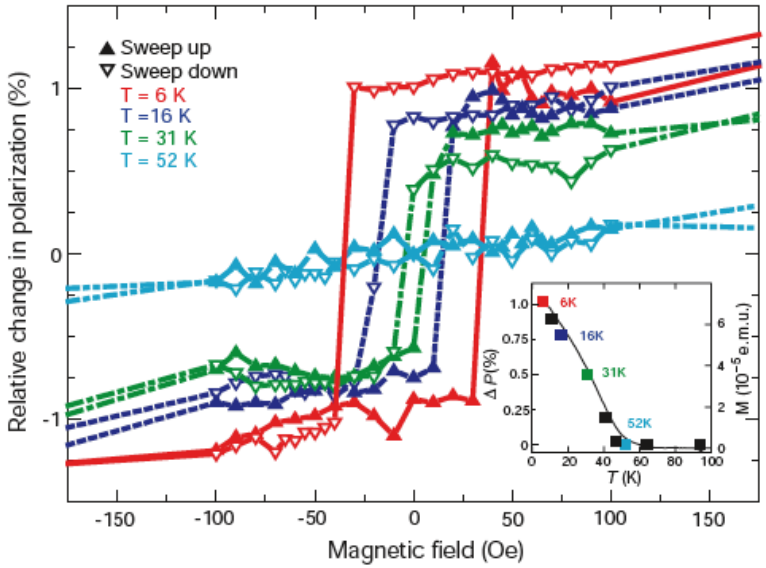

Figure 2 Hysteretic electroluminescence polarization is a direct result of spin injection from the ferromagnetic (Ga,Mn)As layer. Shown are relative changes in the energy-integrated (shaded grey area in Fig. 1b) polarization ΔP, at temperatures $T = 6$–52 K, as a function of in-plane field from a device with $d = 140$ nm. $E = 1.34$ eV, $I = 2.8$ mA. Triangles indicate points taken when the field is swept up or down. Inset, the relative remanent polarization (ΔP at $H = 0$ Oe) shown in solid squares at $T = 6$–94 K, and the temperature dependence of the (Ga,Mn)As magnetic moment, measured by a SQUID magnetometer (solid black curve), demonstrating that polarization is proportional to magnetic moment.

Y. Ohno et al., 'Electrical spin injection in a ferromagnetic semiconductor heterostructure',
Nature 402 (1999) 790.

APPLICATION TO REAL MATERIALS

- Crystal:
  - Translation symmetry
  - Band structure
- Alloying and doping
  - Magnetic impurities occupy cation sites randomly.
  - p-type or n-type carrier doping
- Magnetic disorder
  - In the paramagnetic state, magnetic moments are randomly oriented.

Coherent potential approximation (CPA)

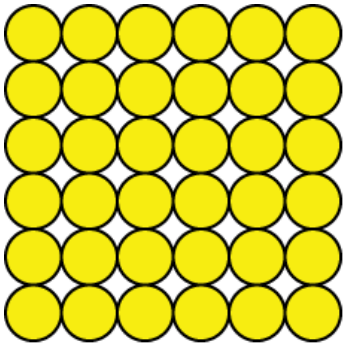

Host semiconductor
(perfect crystal)

Magnetic impurities

Ferromagnetic state

substitutional disorder

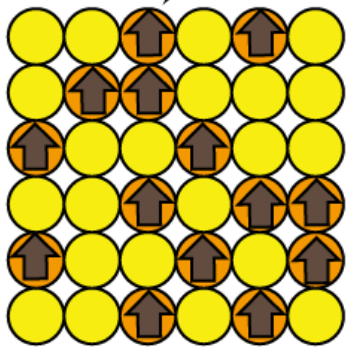

Paramagnetic state

substitutional +
magnetic disorder

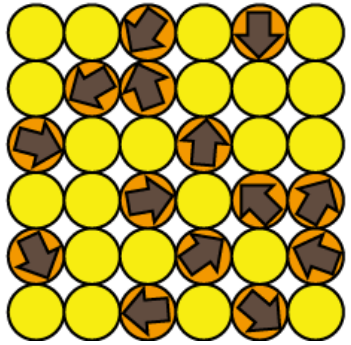

APPLICATION TO DMS SYSTEMS

- Local spin density approximation (LSDA)
- Korringa-Kohn-Rostoker method (KKR)
- Coherent-potential-approximation (CPA)
  ➔MACHIKANEYAMA2002 by Akai

http://kkr.issp.u-tokyo.ac.jp/jp/

(Ga, Mn)As DMS

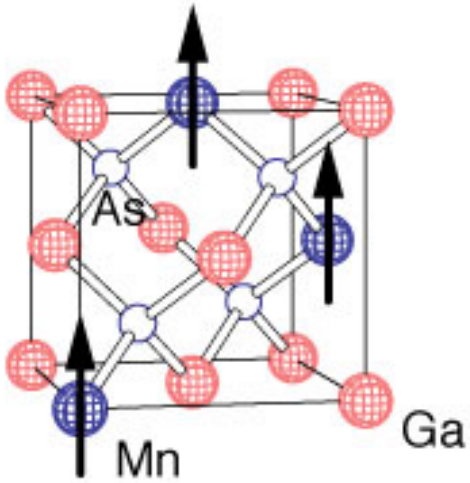

$(Ga_{1-c}, Mn^{\uparrow}_{c})As$

Ferromagnetic state

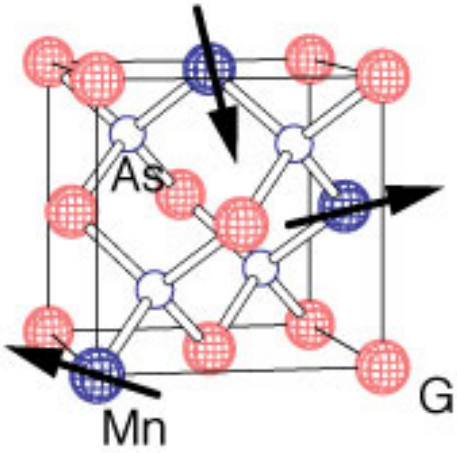

$(Ga_{1-c}, Mn^{\uparrow}_{c/2}, Mn^{\downarrow}_{c/2})As$

Disordered local moment state

Stability of ferromagnetic state: ΔE = TE(DLM) - TE(FM)

Curie temperature in mean field approximation : $k_B T_C = \frac{2\Delta E}{3c}$

T_C^{MFA} OF Mn-DOPED III-V DMS

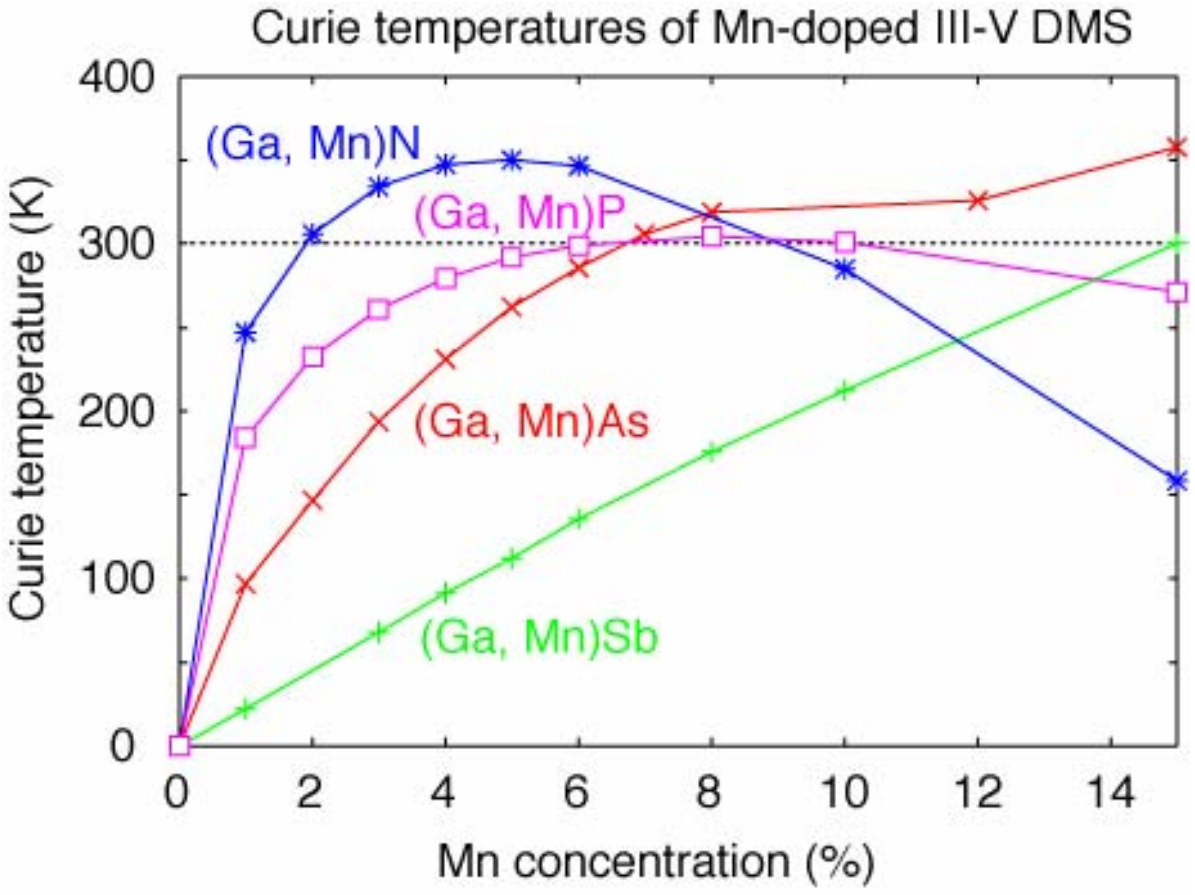

(Ga, Mn)N; Tc ~ √c

(Ga, Mn)Sb; Tc ~ c

↕

Electronic structure

- Origin of the ferromagnetism
  - **double exchange**
  - **p-d exchange**

K. Sato et al., J. Phys. Cond. Matt. 16 (2004) S5491

ELECTRONIC STRUCTURE OF III-V+Mn DMS

K. Sato et al.,
J. Phys. Cond. Matt. 16 (2004) S5491

Impurity band
in the gap → double exchange

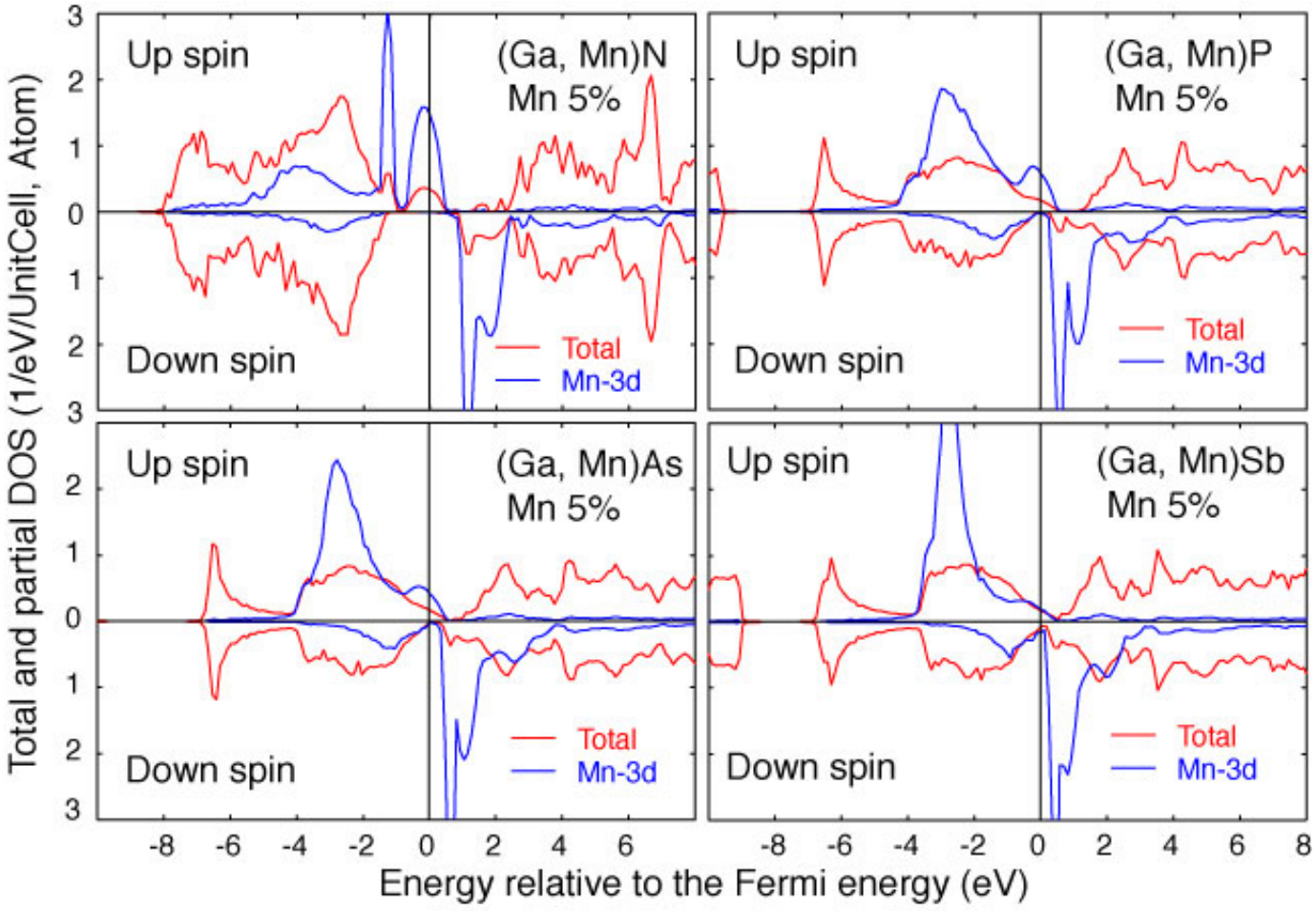

Localized d-states
below valence band → p-d exchange

FERROMAGNETISM IN DMS

Double exchange mechanism [1,2]

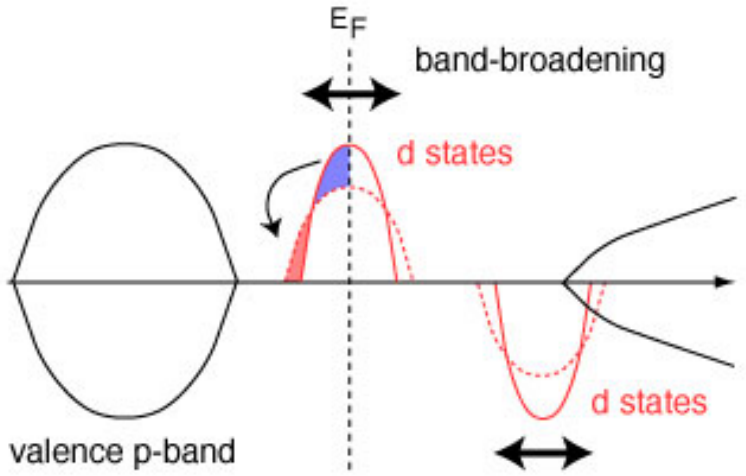

Band energy change in impurity d-band

Band energy gain ~ W ~ $c^{1/2}$

(if E_F is in impurity band)

p-d exchange mechanism [3,4]

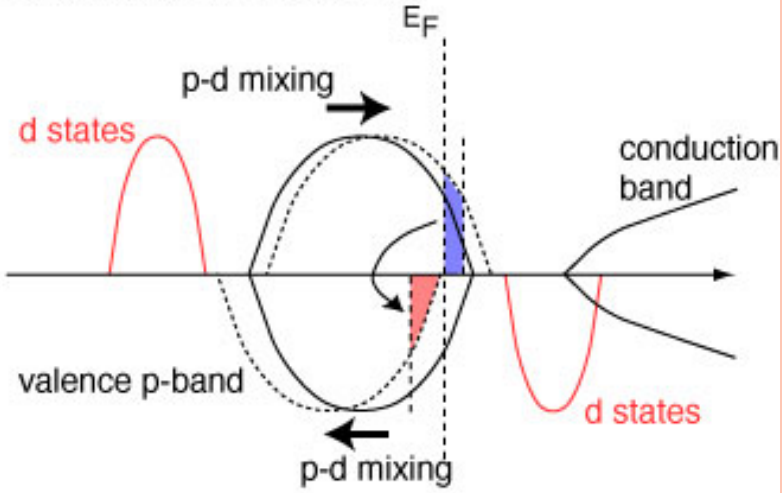

Hole mediated ferromagnetism

Band energy change in valence band

Half-metallic system

Valence band is polarized : -1 μ_B / Mn

Average polarization (mean field) : -c μ_B

Interaction between Mn ions ~ c

1. H. Akai, PRL 81 (1998) 3002. 2. K. Sato and H. K.-Yoshida, Jpn. J. Appl. Phys. 40 (2001) 485.
3. T. Dietl et al., Science 287 (2000) 1019. 4. J. Kanamori and K. Terakura, J. Phys. Soc. Jpn. 70 (2001) 1433.

CALCULATION OF EXCHANGE INTERACTIONS

- Magnetic force theorem
- Mapping on effective Heisenberg model

$$H = -\sum_{i \neq j} J_{ij} \boldsymbol{e}_i \cdot \boldsymbol{e}_j$$

J_{ij}: exchange interaction
e_i: direction of the moment

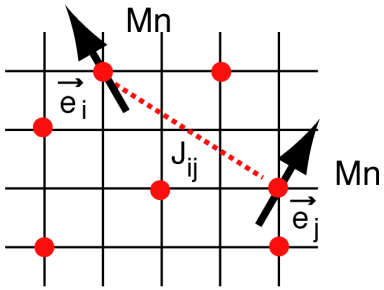

Mn random distribution

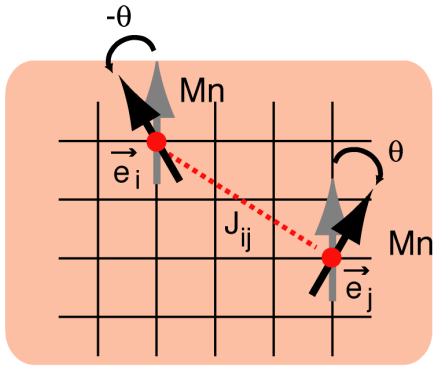

CPA medium

$$J_{ij} = \frac{1}{4\pi} \mathrm{Im} \int^{\varepsilon_F} d\varepsilon \, \mathrm{Tr} \left[\Delta_i(\varepsilon) \tau^{\uparrow}_{ij}(\varepsilon) \Delta_j(\varepsilon) \tau^{\downarrow}_{ji}(\varepsilon) \right]$$

$$\begin{cases} \Delta_i(\varepsilon) = t^{-1}_{i\uparrow}(\varepsilon) - t^{-1}_{i\downarrow}(\varepsilon) \\ \tau_{ij}(\varepsilon) = \left[t^{-1}(\varepsilon) - \tilde{t}^{-1}(\varepsilon) + \tilde{\tau}^{-1}(\varepsilon) \right]^{-1}_{ij} \\ \tilde{\tau}_{ij}(\varepsilon) = \sum_{\vec{k}} \left[\tilde{t}^{-1}(\varepsilon) - g(\vec{k}, \varepsilon) \right]^{-1} \exp\{ i \vec{k} \bullet (\vec{R}_i - \vec{R}_j) \} \end{cases}$$

t: single site t-matrix
τ: scattering path operator
$\tilde{t}$: cpa single site t-matrix
$\tilde{\tau}$: cpa scattering path operator
$\vec{R}$: lattice vector
g: KKR structure constant

EXCHANGE INTERACTIONS IN DMS

K. Sato et al., PRB 70 (2004)201202

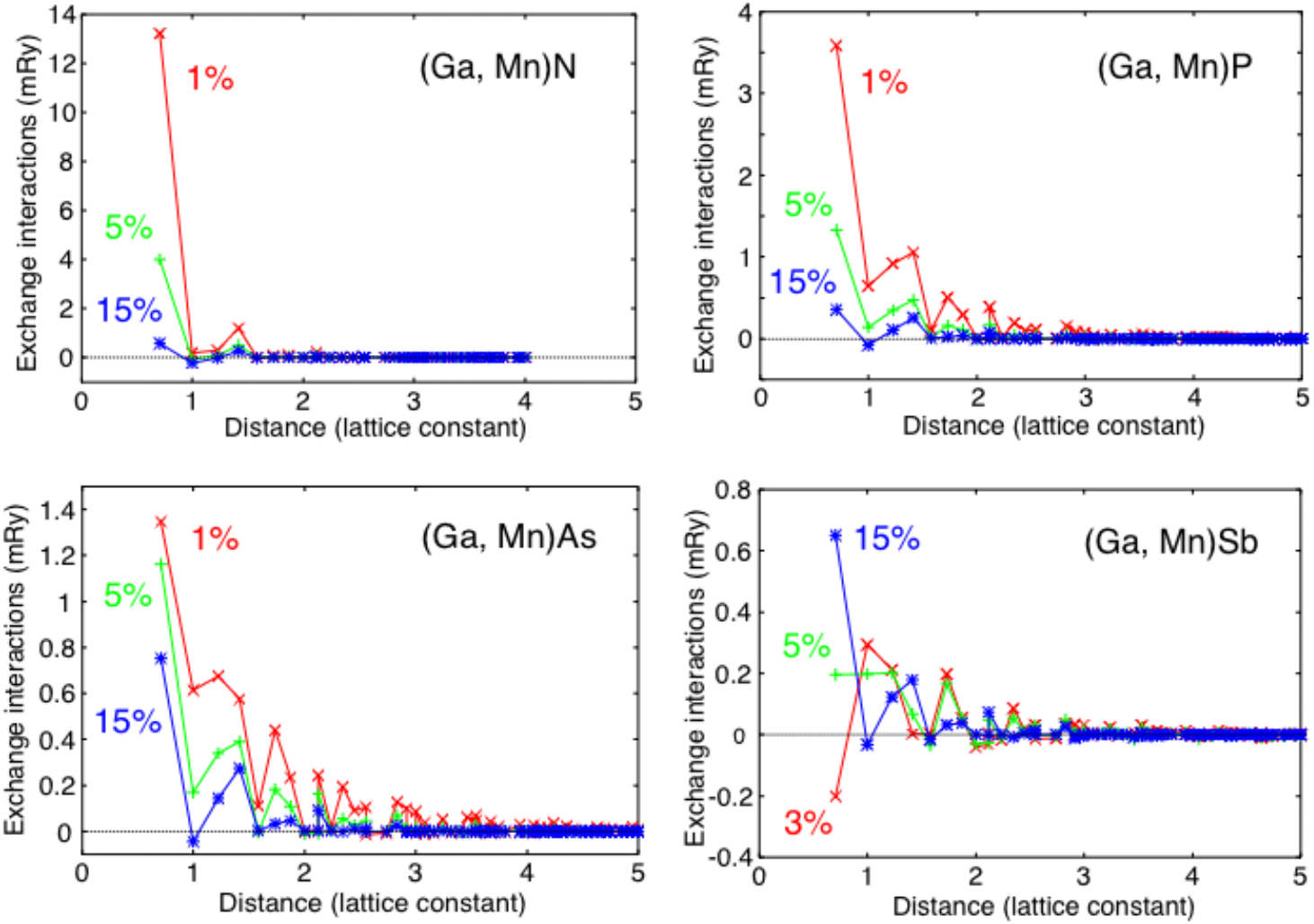

- double exchange system (Ga, Mn)N → strong, but short-range interactions
- p-d exchange system (Ga, Mn)Sb → weak, but long-range interactions

MAGNETIC PERCOLATION PROBLEM

L. Bergqvist et al. PRL (2004)
K. Sato et al., PRB 70 (2004)201202

- 2D square lattice with nearest neighbor interaction.

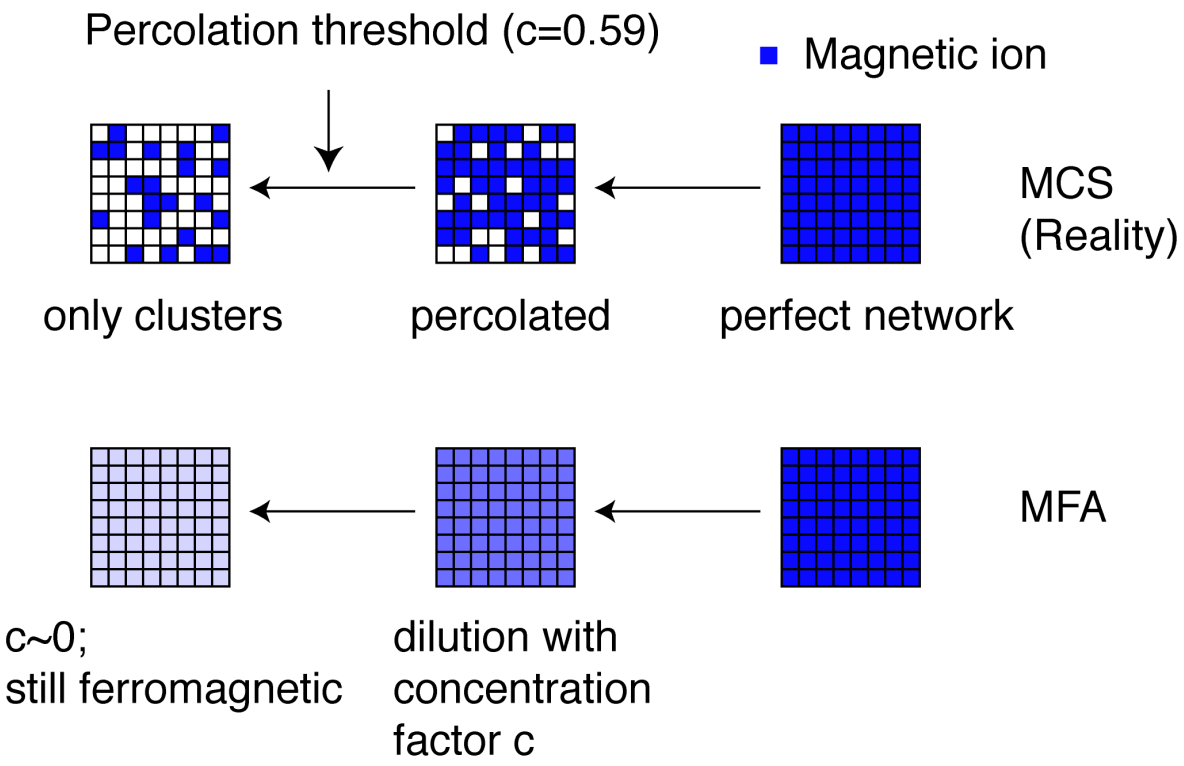

lattice	percolation threshold
square	0.59
triangle	0.50
diamond	0.43
sc	0.31
bcc	0.25
fcc	0.20

D. Stauffer and A. Aharony,
'Introduction to Percolation Theory'
Taylor & Francis, London, 1994

Short ranged interaction → Ferromagnetism is suppressed below the percolation threshold

NEAREST NEIGHBOR HEISENBERG MODEL

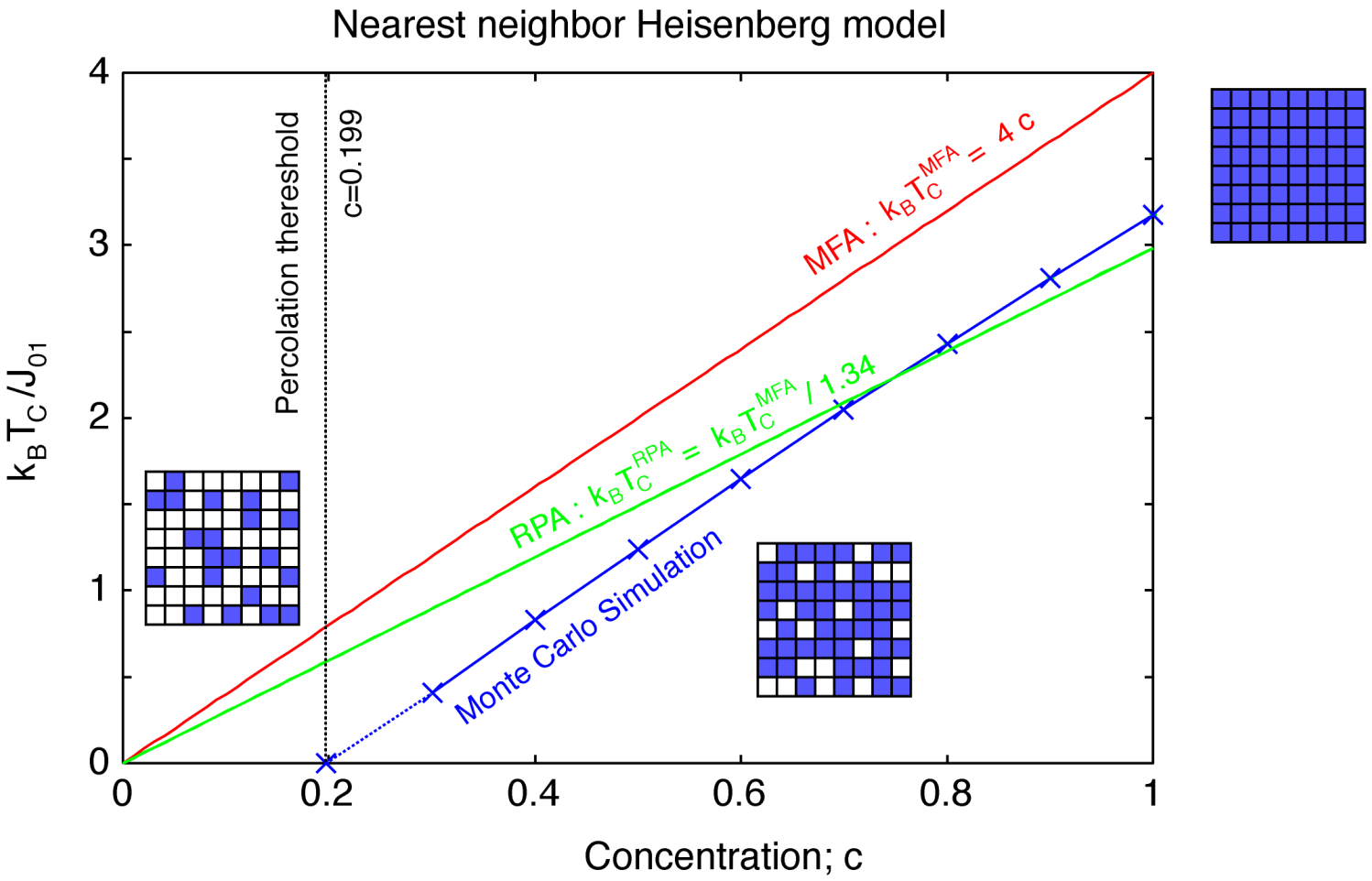

- c~1, MFA values are reasonable
- Ferromagnetism disappears below the percolation threshold

MONTE CARLO SIMULATION

Thermal average of physical observable A

$$< A > = \frac{1}{Z} \int dx \exp [-H(x) / k_B T] A(x) = \frac{\sum_{i=1}^{M} \exp [-H(x_i) / k_B T] A(x_i)}{\sum_{i=1}^{M} \exp [-H(x_i) / k_B T]}$$

Z: partition function k_B : Boltzmann constant
H: model Hamiltonian T: temperature

K. Binder and D. W. Heermann,
'Monte Carlo simulation in statistical Physics'
Berlin, Springer, 1992

Metropolis algorithm ..... efficient sampling technique in the phase space

1) Prepare a simulation box.

$$H = - \sum_{i \neq j} J_{ij} \vec{e}_i \cdot \vec{e}_j$$

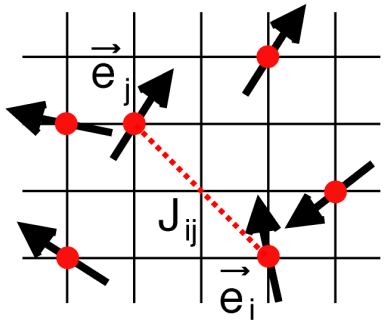

2) Choose a site i, and calculate the energy change ΔE due to a random rotation of the magnetic moment.

3) Generate random number r between 0 and 1.

4) If $r < \exp [-\Delta E/k_B T]$, rotate the moment.

5) Analyze the resulting configuration and store the property for the averaging.

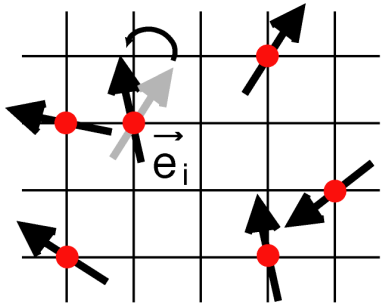

Exact T_C values taking disorder effect fully into account

T_C BY MONTE CARLO

L. Bergqvist et al., PRL (2004)
K. Sato et al., PRB 70 (2004)201202,
T. Fukushima et al., JJAP 43 (2004) L1416

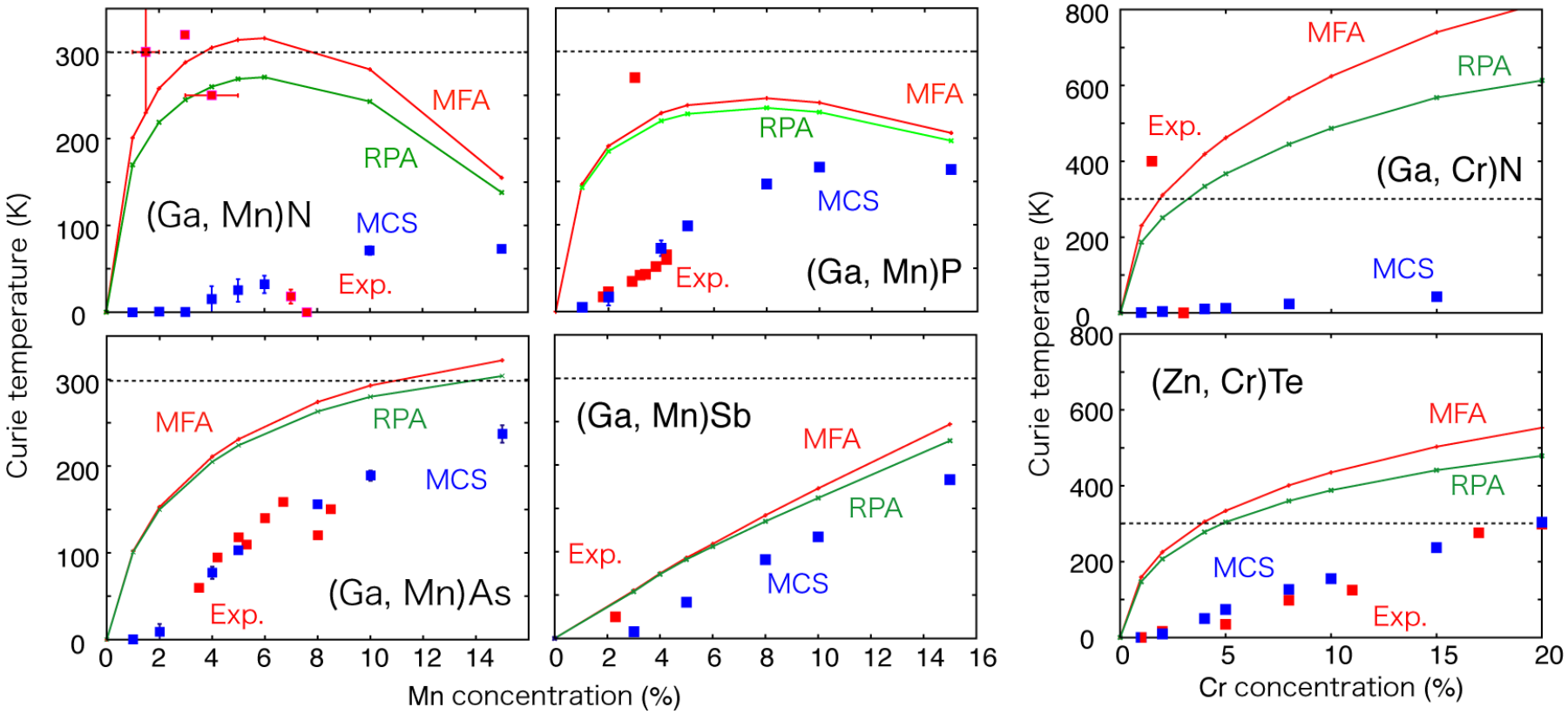

Experimental values:
1. Reed et al. APL 79 (2001) 3473. 2. Thaler et al. APL 80 (2002) 3964. 3. Theodoropoulou et al. APL (2001) 3475. 4. Overberg et al. APL 79 (2001) 1312.
5. Ploog et al. J. Vac. Sci. Technol. B21 (2003) 1756. 6. Scarpulla et al. Physica B340 (2003) 908. SSC 140 (2006) 443 7. Theodoropoulou et al. PRL 89 (2002) 107203.
8. Matsukura et al. PRB 57 (1998) R2037. 9. Edmonds et al. APL 81 (2002) 4991. 10. Ku et al. APL 82 (2993) 2302. 11. Edmonds et al. PRL 92 (2004) 37201.
12. Abe et al. Physica E7 (2000) 981. 13. Hashimoto et al. J. Cryst. Growth 251 (2003) 327. 14. Yamaguchi et al. JJAP 43 (2004) L1312.
15. Saito et al. PRL 90 (2003) 207202. 16. Ozaki et al. Phys. Stat. Sol. 1 (2004) 957.

Reasonable agreement with experiments.

For low concentration, high-T_C can not be expected.(**magnetic percolation**)

Origin of high-T_C phases → **Inhomogeneity**

OUTLINE

- **Introduction**
  - Spintronics, dilute magnetic semiconductors (DMS)
  - Why we need MACHIKANEYAMA ?
    - Disordered systems
    - Finite temperature magnetism
- **Dilute magnetic semiconductors**
  - Origin of the ferromagnetism in DMS
  - Magnetic interactions in DMS
  - Practical and accurate T_C calculation for DMS
  - **Why high-T_C is so difficult ? … magnetic percolation**
- **Inhomogeneity in DMS**

K. Sato et al.,
First-principles theory of dilute magnetic semiconductors, Rev. Mod. Phys., 82 (2010) 1633.
T. Dietl et al.,
Spinodal nanodecomposition in semiconductors doped with magnetic impurities, Rev. Mod. Phys. 87 (2015) 1311.

INHOMOGENEOUS IMPURITY DISTRIBUTION IN DMS

Review: A. Bonnani,
Semicond. Sci. Technol. 22 (2007) R41

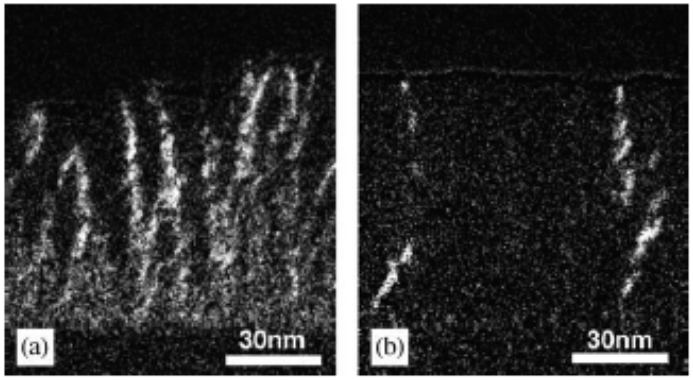

Fig. 1. Energy-filtered electron micrographs showing Cr segregation in Al(Cr)N films grown at 700°C: (a) 7% Cr-doped AlN; (b) 2.5% Cr-doped AlN.

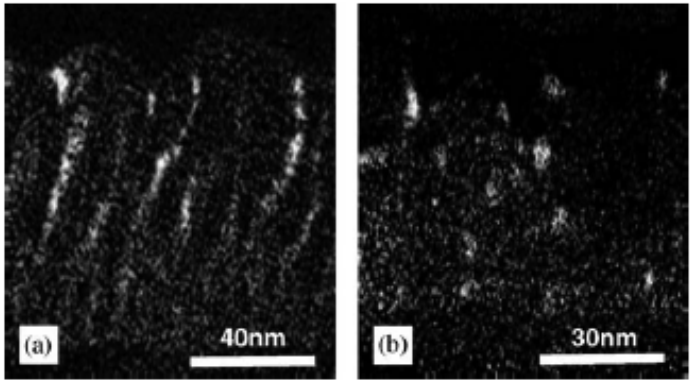

Fig. 2. Energy-filtered electron micrographs showing Cr distribution for 4% Cr-doped AlN grown at different substrate temperatures: (a) 700 °C; (b) 800 °C.

Gu et al., JMMM 290-291(2005)1395.

- MBE
- (Al, Cr)N, Cr 7%, Tc>900K
- (Ga, Cr)N, Cr 3%, Tc>900K
- TEM, EELS
- One-dimensional Cr-rich region: Ferromagnetic
- Spherical clusters:not FM

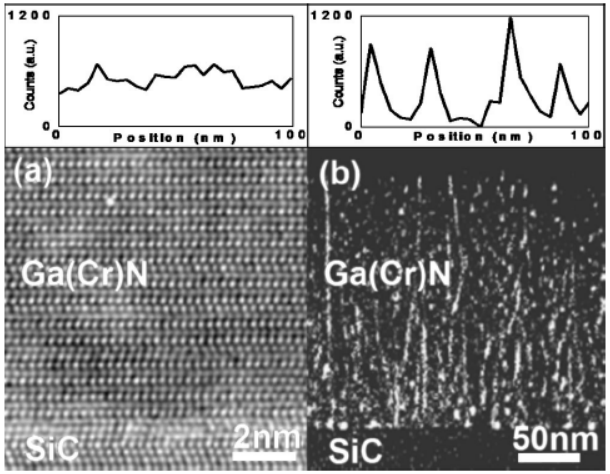

FIG. 3. (a) HRTEM image and (b) energy-filtered TEM image showing Cr distribution in GaN film grown at 775 and 825 °C, respectively. EELS line profile analysis of Cr is shown as inset.

Singh et al., APL 86 (2005)12504

SELF-ORGANIZED NANO-COLUMN IN GeMn

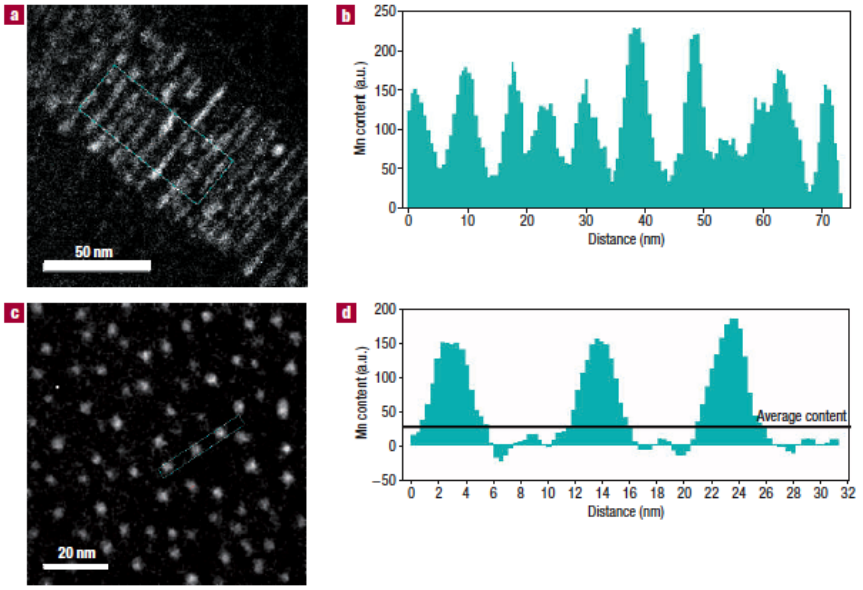

Figure 2 Mn chemical maps and Mn profiles derived from electron energy-loss spectroscopy. a,b, Cross-section, **c,d**, plane view. We recorded 16 pictures in the energy range 500–725 eV every 15 eV on both sides of the Mn $L_{1,2}$ absorption edge at 650 eV. The energy background was carefully subtracted using the pre-edge pictures. We followed the same procedure for Ge chemical maps. By comparing the Ge signal in the buffer with the GeMn film, we confirm the average Mn concentration of 6%. The relatively high background signal in **b** is due to nanocolumns that superimpose in the cross-section image, whereas the background signal between nanocolumns in **d** gives an estimation of the noise level in these spectroscopic measurements.

- Mn-doped Ge
- MBE crystal growth
- TEM, EELS analysis
- Average: Mn = 6%
- Self-organized nano-column
  - 3nm diameter
  - 10nm interval
  - Mn concentration ~ 35%
- $T_C > 400$ K

M. Jamet et al., Nature materials 5 (2006) 653
T. Devillers et al., PRB 76 (2007) 205306

GENERALIZED PERTURBATION METHOD

Ducastelle and Gautier: 'Generalized perturbation method'
J. Phys. F6 (1976) 2039

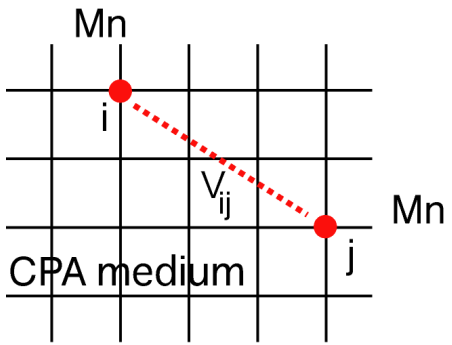

$$H = - \sum_{i \neq j} V_{ij} \, \sigma_i \, \sigma_j$$

$$V_{ij} = V_{ij}^{AA} + V_{ij}^{BB} - 2V_{ij}^{AB}$$

V_{ij} : Effective pair interaction between site i and j

σ_i : Occupation number

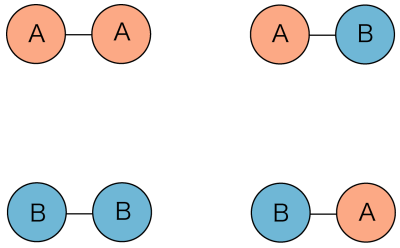

$$V_{ij} = \frac{-2}{\pi} \, \mathrm{Im} \int^{\varepsilon_F} d\varepsilon \, \mathrm{Tr} \left[\Delta_i(\varepsilon) \tau_{ij}(\varepsilon) \, \Delta_j(\varepsilon) \, \tau_{ji}(\varepsilon) \right]$$

$$\begin{cases} \Delta_i(\varepsilon) = X_A^i(\varepsilon) - X_B^i(\varepsilon) \\ \tau_{ij}(\varepsilon) = \sum_{\vec{k}} \left[t^{-1}(\varepsilon) - g(\vec{k}, \varepsilon) \right]^{-1} \exp\{ i \vec{k} \bullet (\vec{R}_i - \vec{R}_j) \} \end{cases}$$

X: single site scattering-matrix
τ: scattering path operator
$\vec{R}$: lattice vector
g: KKR structure constant

Turchi et al., PRL 67 (1991) 1779.

EFFECTIVE PAIR INTERACTIONS IN DMS

K. Sato et al., JJAP 44 (2005) L948, 45 (2006) L 416

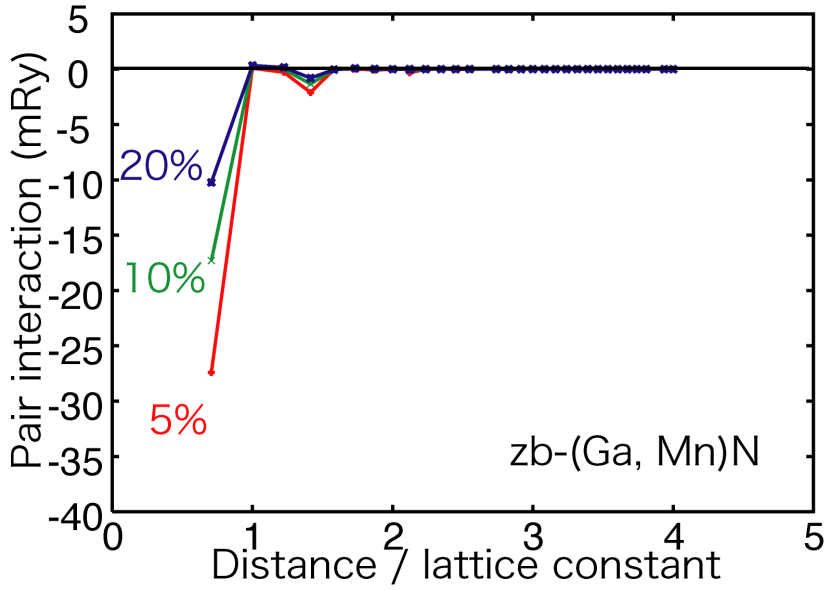

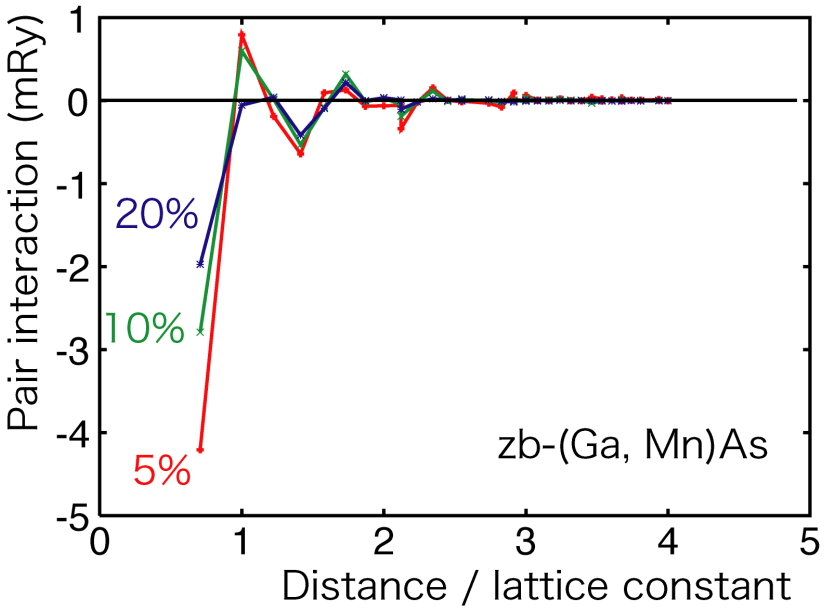

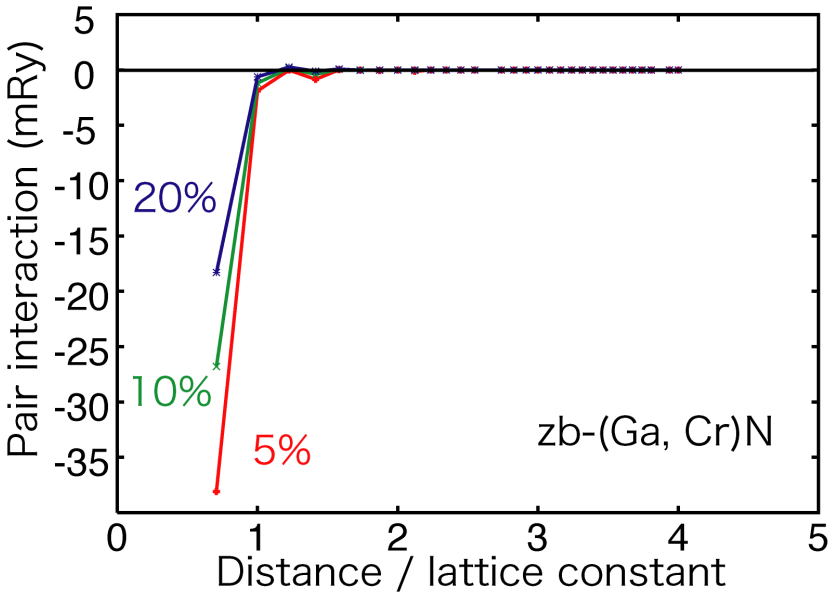

- Effective attractive interactions between nearest neighbors

  → phase separation

- Similar results
  - M. van Schilfgaarde et al., PRB 63 (2001) 233205
  - H. Raebiger et al., JMMM 290-291 (2005) 1398
  - J. Osorio-Guillen et al., PRB 74 (2006) 35305

LAYER BY LAYER GROWTH CONDITION

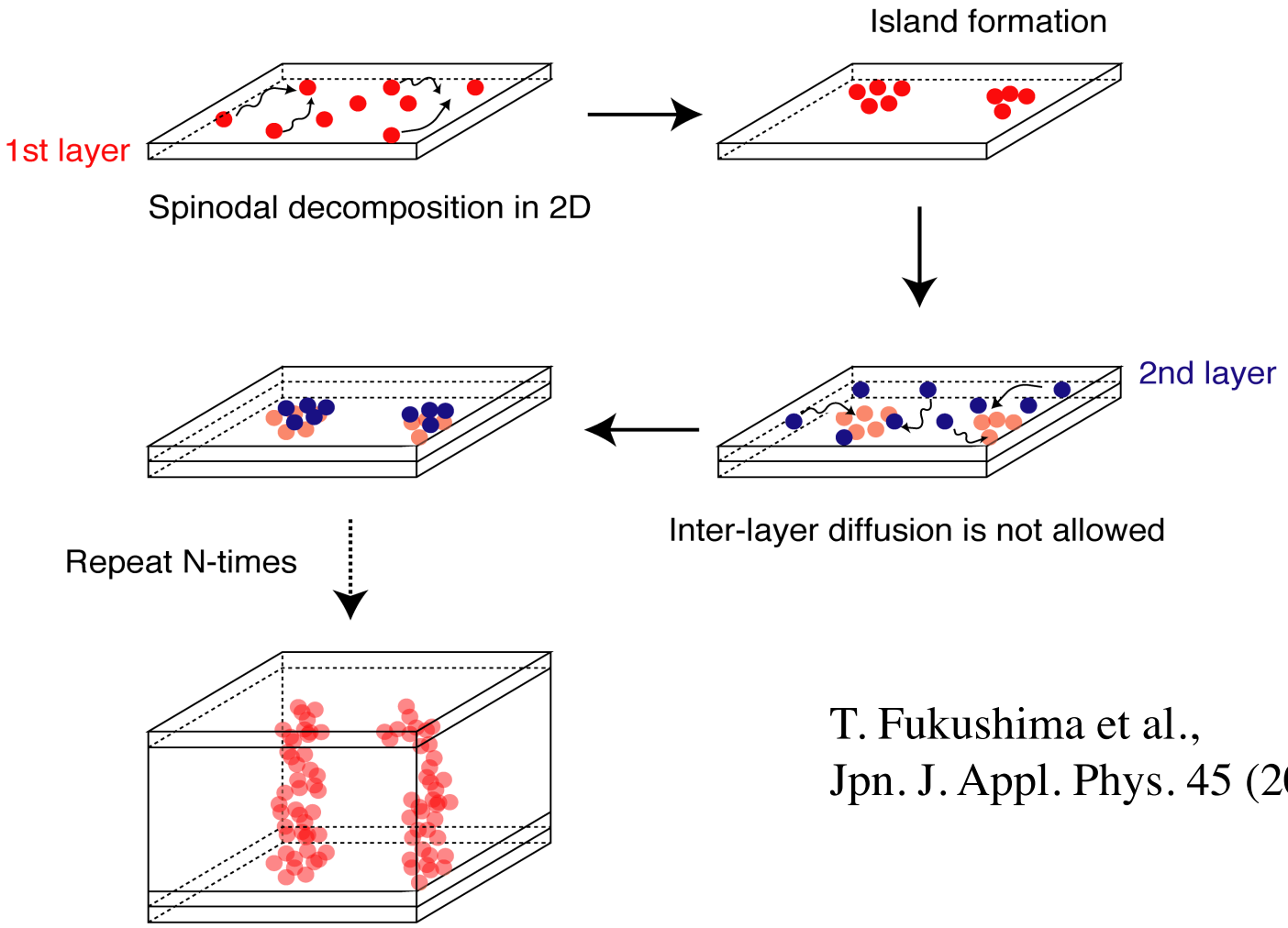

T. Fukushima et al.,
Jpn. J. Appl. Phys. 45 (2006) L416

- Quasi-one dimensional structure due to the spinodal nano-decomposition under the layer-by-layer growth condition
- Large clusters for low concentrations

LAYER BY LAYER GROWTH SIMULATION

T. Fukushima et al., Jpn. J. Appl. Phys. 45 (2006) L416

(Zn, Cr)Te, Cr 5%

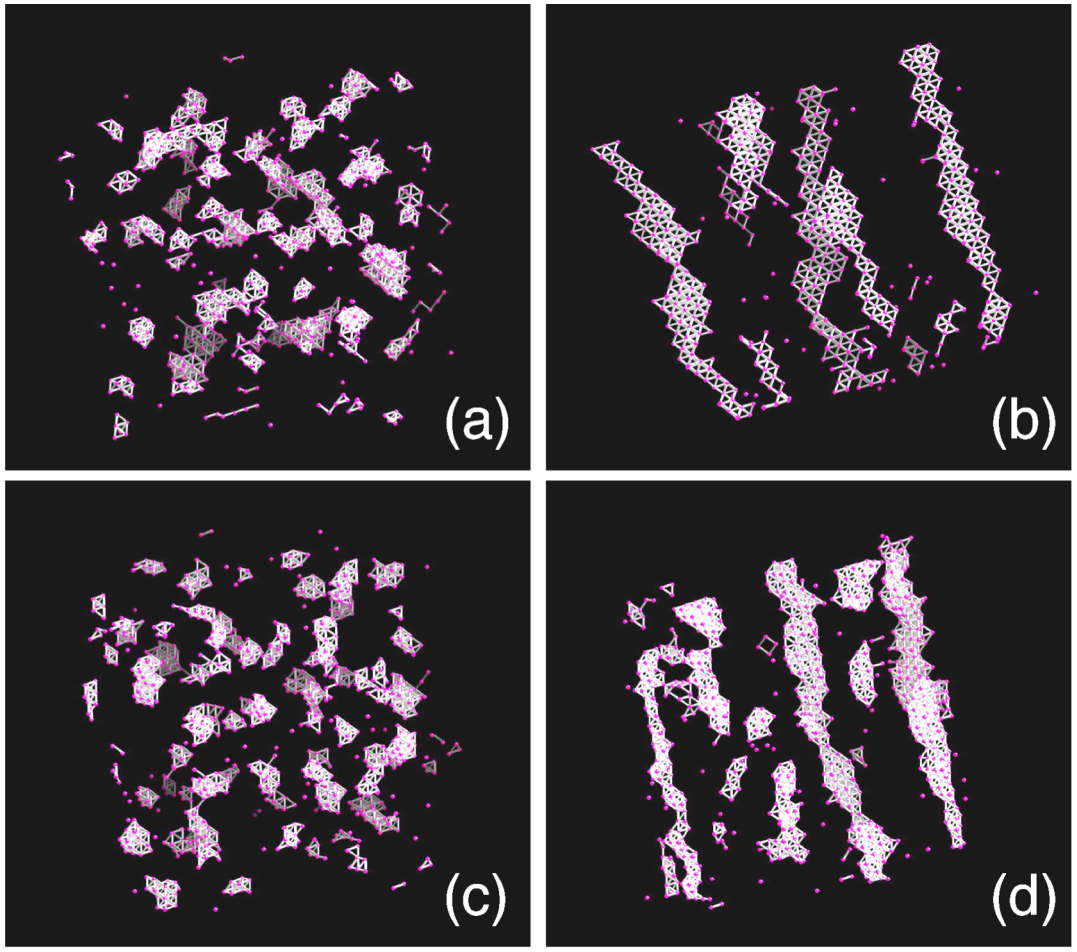

(Ga, Mn)N, Mn 5%

- Spinodal nano-decomposition in 3D
  - Small clusters
  - No percolation
  - Super paramagnetism
- Layer-by-layer condition
  - One dimensional fragments
  - Large clusters
  - Large blocking temperature

SUPER-PARAMAGNETIC BLOCKING PHENOMENA

Finite relaxation time to flip the magnetization due to the energy barrier caused by the anisotropy
→ Hysteretic behavior

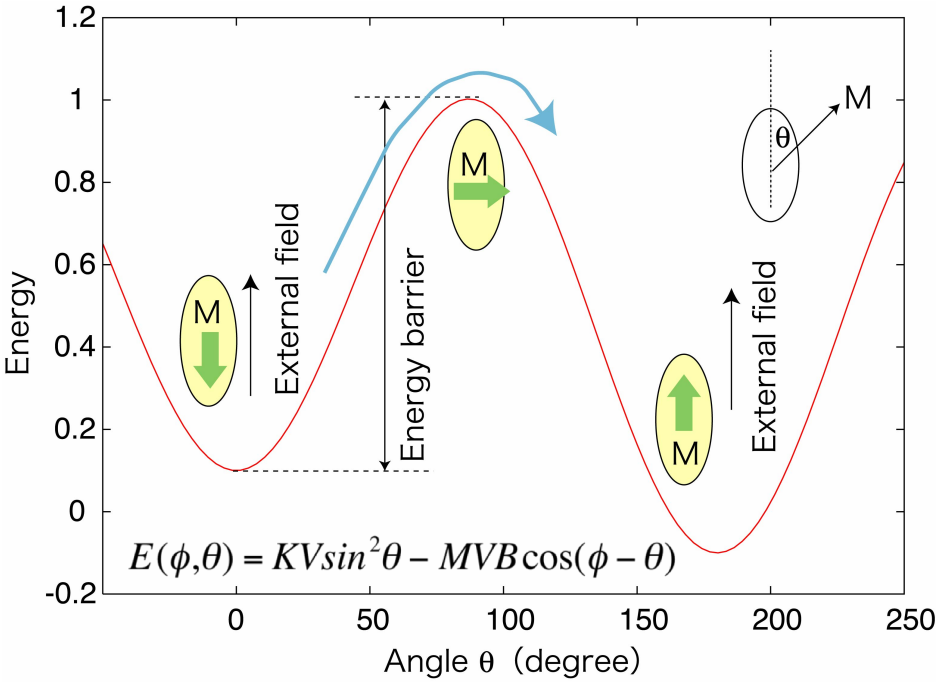

K: Anisotropy, *V*: volume,
M: moment, *B*: external field

K. Sato et al., Jpn. J. Appl. Phys. 46 (2007) L682

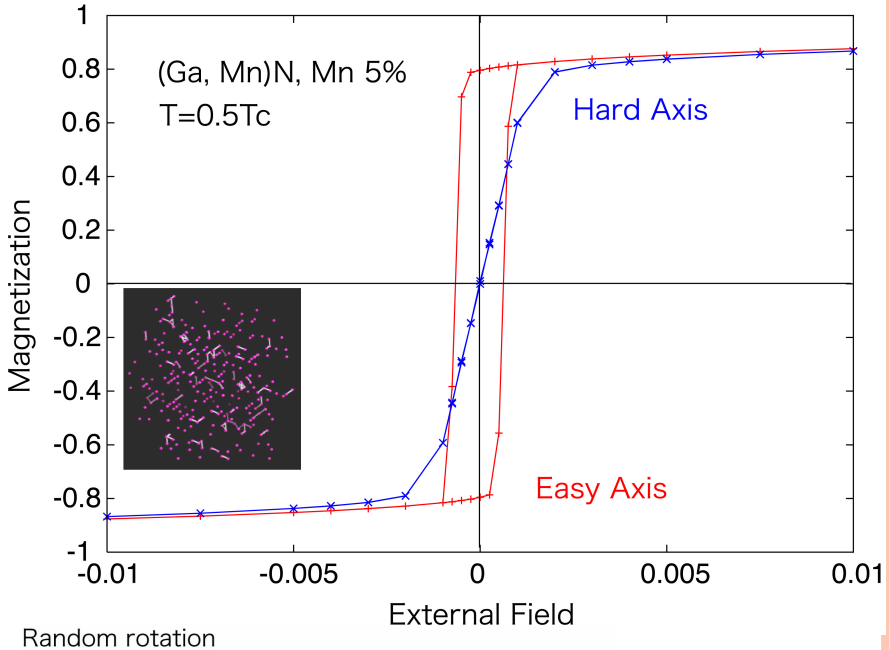

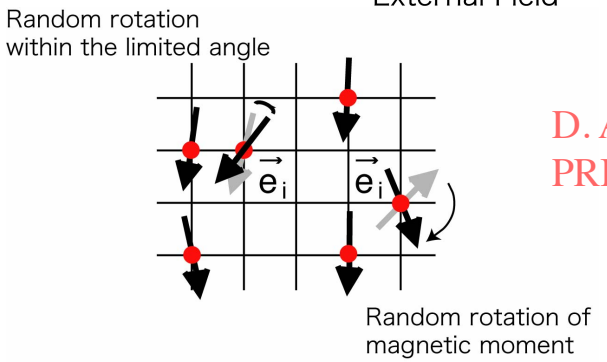

D. A. Dimitrov et al.,
PRB 54 (1996) 9237

- Hysteresis
- Anisotropy constant → parameter

SIMULATION OF BLOCKING PHENOMENA IN DMS

K. Sato et al., Jpn. J. Appl. Phys. 46 (2007) L682

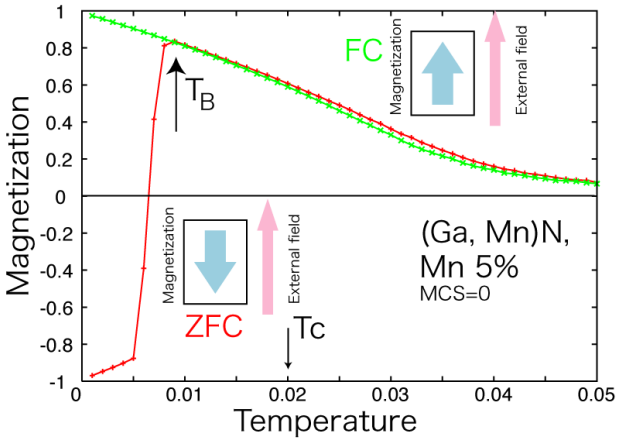

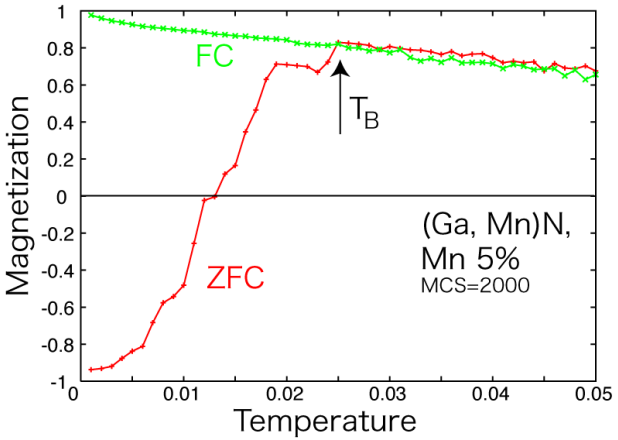

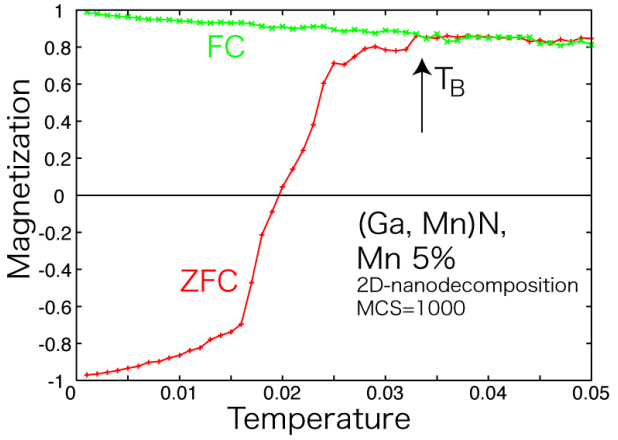

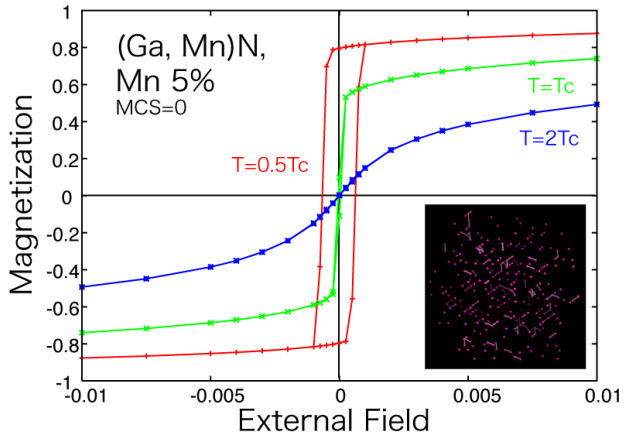

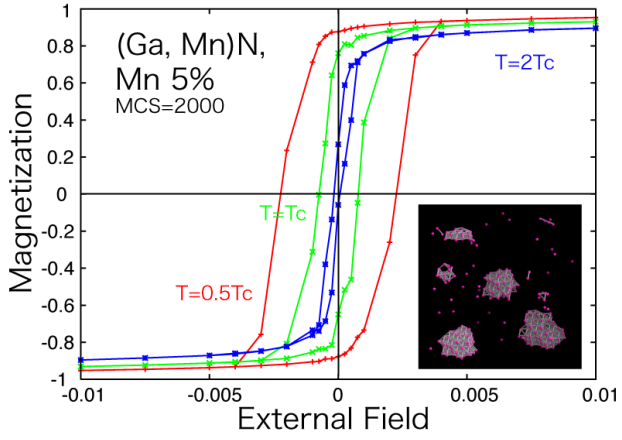

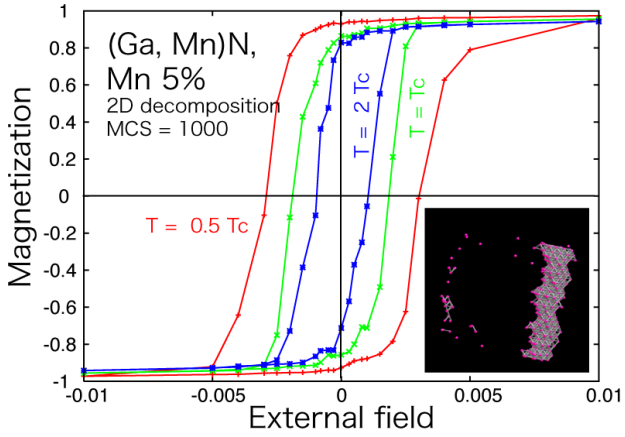

- Homogeneous distribution
  - Above T_C → no hysteresis
- Large cluster → ferromagnetic behavior at high temperature

SUMMARY

- **Application of MACHIKANEYAMA to DMS**
  - Disordered state … KKR-CPA
  - Finite temperature magnetism
    → DLM state, Mapping on Heisenberg model

- **Ferromagnetism in DMS**
  - Impurity band in the gap
    → **double exchange** → short range interaction
  - Localized moment
    → **p-d exchange** → long range interaction
  - Low concentration, Low T_C (**Magnetic percolation problem**)

- **Inhomogeneous DMS**
  - **Phase separation in DMS**
  - **Super-paramagnetism, blocking phenomena**